Fuel 316 (2022) 123387

Contents lists available at ScienceDirect

Fuel

journal homepage: www.elsevier.com/locate/fuel

Full Length Article

Exhaust emissions from a prototype non-road natural gas engine

Petteri Marjanen [a], Niina Kuittinen [a,*], Panu Karjalainen [a], Sanna Saarikoski [b], Mårten Westerholm [c], Rasmus Pettinen [c], Minna Aurela [b], Henna Lintusaari [a], Pauli Simonen [a], Lassi Markkula [a], Joni Kalliokoski [a,d], Hugo Wihersaari [d], Hilkka Timonen [b], Topi Rönkkö [a]

[a] Aerosol Physics Laboratory, Physics Unit, Faculty of Engineering and Natural Sciences, Tampere University, Korkeakoulunkatu 3, PL692, 33014 Tampere, Finland
[b] Atmospheric Composition Research, Finnish Meteorological Institute, P.O. BOX 503, FI-00101 Helsinki, Finland
[c] VTT Technical Research Centre of Finland, PL 1000, 02044 VTT, Espoo, Finland
[d] AGCO Power, Linnavuorentie 8-10, FI-37240 Linnavuori, Finland

ARTICLE INFO

Keywords:
Gas engine
Natural gas
Lubrication oil
Exhaust emission
Black carbon
Non-road

ABSTRACT

Since gas engines are considered a future solution to improve air quality and to mitigate climate impacts, there is an urgent need to understand their emissions. The aim for this study was to understand the phenomena affecting the formation of particulate emissions of a non-road natural gas engine. To achieve this, the engine's exhaust emissions were characterized under different operating conditions. The regulated pollutants (gaseous CO, HC, and NO_x; particulate matter (PM) and particle number (PN)) were determined experimentally and a detailed characterization of particulate pollutants over a wide particle size range (particles down to 1.2 nm) was conducted with state-of-the-art instrumentation considering both physical and chemical properties of the exhaust aerosol. The test engine was a prototype non-road spark-ignited natural gas engine, which was studied over the non-road steady test cycle (NRSC). The role of the three-way catalyst (TWC) was studied by sampling and characterizing the exhaust aerosol both with and without the TWC. The TWC was observed to efficiently remove the vast majority of the regulated gaseous (96% CO, 98% HC, 98% NO_x) and particulate mass emissions (98%). In general, the measured particle number emission factors were highly dependent on the cut-off sizes of the condensation particle counters. Using CPCs with smaller cut-off sizes resulted in higher particle number emission factors. For black carbon (BC), the intermediate engine speed conditions (modes 5–7) led to lower BC emissions than the high speed conditions (modes 1–3). In contrast, highest BC emissions on a work basis were observed during idling. TWC did not influence BC levels. Without the TWC, PM was comprised mostly of organic compounds (70–100%). Downstream of the TWC, the majority of PM was, depending on the load, composed of organic compounds, sulfate, or black carbon. A statistical source apportionment based on mass spectra revealed that the PM_1 was mostly related to unburned and burned lubricating oil, indicating a minor role of fuel in PM formation.

1. Introduction

Global warming is currently one of the great challenges of our society. It is largely caused by the use of fossil fuels, and particularly, anthropogenic emissions of carbon dioxide (CO_2), methane (CH_4), and black carbon (BC) [1]. Climate warming mitigation requires urgent actions to decrease the emissions of these compounds, which has led to an increased need to develop new technical solutions, especially for engines

Abbreviations: BC, Black carbon; CPC, Condensation particle counter; CVS, Constant volume sampling system; DR, Dilution ratio; H/C ratio, Hydrogen-to-carbon ratio; NRMM, Non-road mobile machinery; MSS, Micro soot sensor; PM, Particulate matter; PN, Particle number; PMP, Particle measurement program; PSM, Particle size magnifier; PTD, Porous tube diluter; TWC, Three-way catalyst; SMPS, Scanning mobility particle sizer; UFP, Ultrafine particles ; SP-AMS, Soot-Particle Aerosol Mass Spectrometer.

* Corresponding author.
E-mail addresses: petteri.marjanen@tuni.fi (P. Marjanen), niina.kuittinen@tuni.fi (N. Kuittinen), panu.karjalainen@tuni.fi (P. Karjalainen), sanna.saarikoski@fmi.fi (S. Saarikoski), Marten.Westerholm@vtt.fi (M. Westerholm), Rasmus.Pettinen@vtt.fi (R. Pettinen), Minna.aurela@fmi.fi (M. Aurela), henna.lintusaari@tuni.fi (H. Lintusaari), pauli.simonen@tuni.fi (P. Simonen), lassi.markkula@tuni.fi (L. Markkula), joni.kalliokoski@tuni.fi (J. Kalliokoski), Hugo.Wihersaari@agcocorp.com (H. Wihersaari), Hilkka.Timonen@fmi.fi (H. Timonen), topi.ronkko@tuni.fi (T. Rönkkö).

https://doi.org/10.1016/j.fuel.2022.123387
Received 24 August 2021; Received in revised form 20 December 2021; Accepted 19 January 2022
Available online 1 February 2022

and power production. In general, the climate effects of the strongest climate forcers CO_2, CH_4, and BC are caused by different mechanisms and, importantly, their atmospheric lifetimes differ significantly from each other [1-4]. In addition, because these compounds are frequently emitted from combustion processes simultaneously with compounds having cooling effects on the climate [5,6], their mitigation requires careful investigation of co-emitted compounds and understanding of possible trade-offs in emissions [5,7] and their effects. For instance, the engine emissions of particulate BC are efficiently reduced by filtration [8] which, on the other hand, slightly increases the total CO_2 emissions of engine operation [9]. While the climate effects of greenhouse gas emissions can be assessed by the commonly used carbon footprint concept, the evaluation of the environmental effects of BC may be more complicated [10], due to the various effects of BC both on climate and on human population health [1,3,11-13].

Natural gas and biogas are composed mostly of methane, and they are considered, in general, as one solution to decrease CO_2 emissions from traffic, power production, and heating. This is due to the relatively high hydrogen-to-carbon ratio (H/C ratio) of CH_4 when compared to liquid fossil fuels, which results in lower CO_2 emissions [14], and thus climate warming impacts. The positive impacts of the utilization of gaseous fuels are enhanced with biogases that have renewable sources and thus very low carbon footprint [15]. In addition, the particle emissions of gas engines have been reported to be low when compared to other engine types [16,17], and gas engines can frequently be equipped with three-way catalysts (TWC) that limit their NO_x emissions to the levels of modern diesel and gasoline cars [18]. These benefits of gaseous fuels have increased their utilization as a part of efforts to reduce global warming by reducing the use of fossil fuels. Gas-fueled vehicles are also used to replace diesel and gasoline fueled vehicles to improve air quality because the particle mass and NO_x emissions of gas engines are typically low. For example, using gas-fueled engines in city buses has a clear potential to reduce the particle emissions of traffic [19] and thus also the human exposure to harmful pollutants. This is particularly true for particulate air pollution, represented by particles with a diameter of less than 2.5 μm (PM2.5), which have been frequently linked to adverse health impacts, increased mortality, and morbidity in epidemiological studies [20-22]. Gas-fueled vehicles and mobile machinery are considered to be one solution to improve this problem.

Previous studies [16,17,23-28] have shown that particle emissions from gas-fueled engines are low compared to diesel and gasoline engines without exhaust particle filtration systems. Also, compared to liquid diesel fuels, natural gas is a feasible solution for reducing particle number (PN) emissions from large scale engines [27,29]. However, the particle number emissions of gas-fueled engines can still be important, due to the emissions of particles with relatively small particle sizes. The formation of gas engine exhaust particles has been studied in detail, e.g., by Alanen et al. [25], who reported high numbers of particles in ultrafine particle size range (particle size <100 nm) and especially in sub 10 nm sizes from a passenger car engine modified to run on natural gas under both high and low torque conditions [25]. Their study, conducted with a gas engine without exhaust aftertreatment systems, reported that the exhaust particles were most likely initially formed in the cylinder and grew in the exhaust sampling process by condensation of semi-volatile compounds to larger particle sizes. In a study of a dual fuel marine engine without exhaust aftertreatment [24] that used diesel fuel to ignite natural gas, the results further confirmed the important role of the smallest particles in emissions and indicated that the compounds originating from lubricating oil can also contribute to particle emissions from gas-fueled engines.

Because the gas-fueled engines are recognized as a future solution to improve air quality and to mitigate climate impacts, there is urgent need to understand their emissions. This is true especially regarding the particle emissions that are challenging to understand with respect to their small particle sizes, still unclear formation processes, and complex chemistry. In addition, the particle emissions can be strongly affected by engine and vehicle technologies and by engine operation conditions, and the role of lubricant and catalysts on particle emissions are not yet completely understood. Watne et al. [16] observed high variation in fresh emission factors from compressed natural gas (CNG) vehicles and found that particle mass formed in the atmosphere via exhaust oxidation in relation to fresh emissions could be high for CNG vehicles.

The aim of this study is to understand the phenomena affecting the formation of gaseous and particulate emissions of a natural gas engine. To achieve this, the study characterizes in-detail exhaust emissions for a gas-fueled engine for changing engine operating conditions. The regulated pollutants (carbon monoxide (CO), total hydrocarbons (HC), nitrogen oxides (NO_x), particulate matter (PM) and number of particles>23 nm) were determined experimentally and a detailed characterization of particulate pollutants was conducted over a wide particle size range (down to 1.2 nm) with state-of-the-art instrumentation for measuring both the physical and chemical properties of the exhaust aerosol. The test engine was a prototype, non-road, spark-ignited gas engine, which was studied over the non-road steady test cycle (NRSC). The role of the TWC was studied by sampling and characterizing the exhaust aerosol from the engine both with and without the TWC installed.

2. Materials and methods

2.1. Engine, fuel, and lubricating oil

The engine used in this study was a prototype non-road engine that ran on natural gas. Maximum power during the measurements for the engine was 85.8 kW. The engine applied spark plugs to ignite the premixed natural gas. The studied engine has been developed for future use in non-road working machines, for example in agricultural tractors. It should be noted that the studied engine was a prototype, and before commercialization both the engine and the after-treatment system would be further optimized. In addition, use of gas in agricultural machinery would require fuel availability as well as fitting the working machine with tanks capable of storing enough gas for entire day operation. The exhaust tailpipe of the engine was equipped with a TWC, that could be removed without changing the sampling system position.

The natural gas used to fuel the engine was from the Finnish natural gas network. The natural gas in the Finnish natural gas network is mainly of Russian origin, and 96.8% of its composition was CH_4. The supply line pressure was 3.5 bar, compressed up to 7 bar for engine supply, which would represent the transfer line from tank to the engine in an actual application. The lubricating oil used in the study was Shell Rimula R4 Multi 10 W-30, which is recommended by the manufacturer for use in off-highway applications, such as agricultural tractors and mining operations.

2.2. Engine operating conditions

The studied engine was operated in a test bench according to the steady conditions for the non-road steady test cycle (NRSC, also known as the ISO 8178 C1 test cycle). NRSC for type C1 non-road engines consists of eight at least 10-minute steady driving modes that contain three different engine speeds and several different torque points. The speed and torque values for the studied engine are presented in Table 1.

Table 1
Speed and torque values for the studied engine for the eight driving modes of NRSC. Weighting factors were used for calculating the regulated emission factors [30].

Mode number	1	2	3	4	5	6	7	8
Speed (rpm)	2200				1400			900
Torque (Nm)	350	260	170	35	450	340	220	54
Weighting factor	0.15	0.15	0.15	0.1	0.1	0.1	0.1	0.15

During two of the measured NRSC cycles the engine was equipped with a TWC after-treatment system. To investigate the effect of the TWC, three additional tests were conducted with the TWC uninstalled. The runs with the TWC installed are referred from now on as Tests 1–2 and runs without the TWC as Tests 3–5. Exhaust temperatures and air-to-fuel equivalence ratio (lambda value) were monitored throughout the experiment and the engine was controlled by closed loop lambda control, where a lambda value between 0.995 and 1.005 was continuously targeted. In general, the lambda value stayed around 0.99 in all modes except mode 8, where the lambda value was consistently above the targeted range. Test 1 differed from the other tests in that mode 4 lambda value was also above the targeted range. A lambda value of 1 indicates stoichiometric combustion conditions. Lambda value above 1 indicates that in mode 8 there was more oxygen present than is needed for perfect combustion. Exhaust temperatures upstream and downstream the TWC are shown in Figure S1.

2.3. Sampling system and measurement setup

Measurements were conducted simultaneously applying three parallel sampling systems. Firstly, from the undiluted exhaust, secondly after the ISO 8178 dilution protocol (CVS constant volume sampling tunnel), and thirdly after the partial flow dilution system. Various instruments and dilution methods used in the experiments are presented in Fig. 1 and Table 2.

Most of the particle instruments were located after a partial flow dilution system that consisted of a porous tube diluter (PTD) [31,32] combined with a residence time tube and an ejector diluter (ED)[33]. Dilution ratios (DR) for the partial flow dilution system were determined by measuring CO_2 concentrations of the sample at different dilution stages. A DR of 12 was targeted for the PTD, resulting in a total DR of 100–107 for the PTD + ED. The PTD sampling method has been demonstrated to mimic real-life dilution with ambient air with respect to particle formation [34]. It should be noted, that unlike the particle measurement programme (PMP) method, PTD sampling, in which 30 °C air is used in the first dilution step, allows nucleation and condensation

Table 2
Measured parameters, details about instruments, and information about dilution.

Measurement	Instrument	Producer	Dilution method
CO_2	SIDOR	Sick Maihak AG	PTD
CO_2	LI-840A	LI-COR Biosciences UK	PTD + ED
CO_2	AMA i60	AVL	Undiluted exhaust
CO, CO_2, HC, NO_x	AMA i60	AVL	CVS
PM	Filter collection	AVL	CVS + secondary diluter
PN > 23 nm non-volatile	A23 CPC	Airmodus	CVS + DEED
PN > 23 nm	A23 CPC	Airmodus	PTD + ED + bridge diluter
PN > 10 nm	A20 CPC	Airmodus	PTD + ED + bridge diluter
PN > 1.2 nm	PSM + A20 CPC	Airmodus	PTD + ED + bridge diluter
PN > 2.5 nm	3776 UCPC	TSI	PTD + ED + bridge diluter
PN > 5 nm	MAGIC CPC	Aerosol Devices Inc.	PTD + ED + bridge diluter
Particle number size distribution	Nano-SMPS (3082 electrostatic classifier 3085 Nano DMA + 3756 CPC)	TSI	PTD + ED
BC	Micro Soot Sensor	AVL	Internal dilution
BC	Aethalometer AE33	Magee Scientific	PTD + ED
BC	microAeth MA200	AethLabs	PTD + ED
BC	MAAP	Thermo Scientific	PTD + ED
Chemical composition	SP-AMS	Aerodyne	PTD + ED

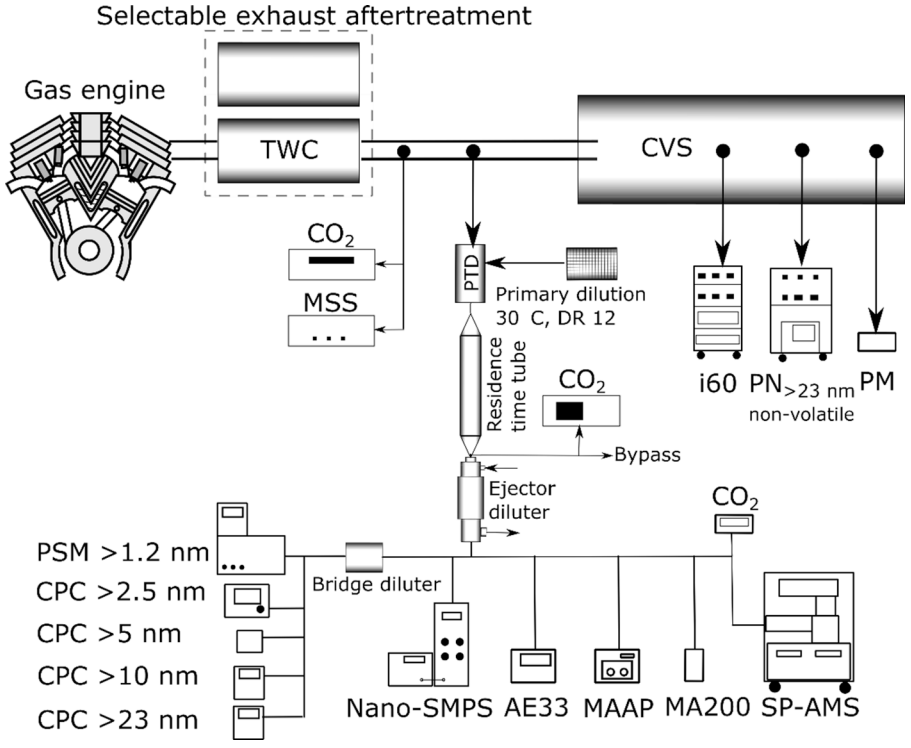

Fig. 1. Schematic of the measurement setup.

of gaseous precursors to the particle phase. Thus, comparison of particle results obtained after different dilution methods can give insight of the particle formation process.

Gaseous emissions (CO, CO_2, HC, and NO_x) were measured with an AVL AMA i60 exhaust measurement system (i60). Particulate matter (PM) and number of non-volatile particles with diameter above 23 nm ($PN_{>23\ nm\ non\text{-}volatile}$) were measured according to the ISO 8178 protocol. A Dekati Engine Exhaust Diluter (DEED) including removal of volatile particles was used to dilute the sample for $PN_{>23\ nm\ non\text{-}volatile}$ measurement. Particle number emissions were measured with multiple parallel condensation particle counters (CPC) with a variety of cutoff values. The MultiCPC system, including 3 CPCs with cut-off sizes at 1.2 nm (after the particle size magnifier, PSM), 10 nm, and 23 nm, was paired with an ultrafine condensation particle counter (UCPC) with a cut-off size at 2.5 nm. In addition, particle number was measured with a water-based CPC with cut size at 5 nm [35]. Bridge diluters were used upstream these CPCs resulting in total DR of 22 500 without TWC and 7000 in measurements with TWC. The particle number size distribution was characterized with a scanning mobility particle sizer (SMPS). BC emissions were studied simultaneously with a Micro Soot Sensor (MSS), an aethalometer (AE33), microAeth (MA200), multi angle absorption photometer (MAAP), and soot particle aerosol mass spectrometer (SP-AMS). The measurement principle of the MSS is based on the photo-acoustic spectroscopy (PAS) method, where a modulated laser beam causes a sound pressure wave detected by a microphone. AE33 and MA200 measure the concentration of black carbon by measuring the transmission of light through a filter tape containing the sample. MAAP determines BC concentration by measuring light transmitted and scattered by the sample.

The SP-AMS [36] was used to measure the chemical composition of the submicron aerosol particles. The SP-AMS has an aerodynamic lens to guide particles (between 50 nm and 1 μm in size) as a narrow particle beam to vacuum chamber, and five vacuum pumps to generate the needed vacuum ($\sim 1 \times 10^{-5}$ Torr). The instrument has a dual vaporizer. An intracavity laser vaporizer (1064 nm) vaporizes particles containing light-absorptive compounds (BC, metals, absorptive organics) while a tungsten oven vaporizes non-refractive PM. Vaporized ions are immediately ionized using 70 eV electron impact (EI) ionization. The ions are introduced into a time-of-flight chamber (effective ion path length L = 1.3 m) and detected with a multichannel plate (MCP) detector. The instrument was calibrated using ammonium nitrate and regal black (BC). Time resolution of measurements was one minute.

The SP-AMS data was analyzed with a Positive Matrix Factorization (PMF) method (CU AMS PMF tool v. 2.08D [37,38]) to separate different types or sources of organics. In order to improve the identification of PMF factors, also refractory BC (C_2^+, C_3^+, C_4^+), sulfate (SO^+, SO_2^+, SO_3^+, HSO_3^+, $H_2SO_4^+$) and zinc ($^{64}Zn^+$) fragments were included in the organic PMF data matrix. A similar approach has been used for example by Carbone et al. [39] and Rivellini et al. [40]. The number of factors was varied from two to five and PMF was applied separately to the data collected without and with the TWC, as well as to the combination of both data sets. The latter approach did not produce any reasonable results and therefore the PMF solutions obtained separately for two data sets were analyzed further. Both without and with the TWC, two factor solutions gave the most realistic results. Similar results were obtained by including only organic fragments. Without the TWC, the mass spectra of both factors were dominated by hydrocarbon fragments and are therefore referred to as hydrocarbon-like organic aerosols (HOA) HOA-1a and HOA-2a. Also, after the TWC the mass spectra of both factors consisted mostly of hydrocarbon fragments and are hereafter called as HOA-1b and HOA-2b. Two factor solutions were tested for the accuracy with bootstrapping tests and multiple seeds that resulted in constant factor profiles and contributions. It should be noted that the data sets for the PMF analysis were small in terms of the number of data points. Without the TWC, the SP-AMS data included 150 1-minute data points (two tests/cycles), whereas with the TWC, the data set contained only 73 1-minute data points (one test/cycle). Regardless of the small data sets, the PMF analysis gave valuable information on the sources of particles produced in gas engines. The results for the CPC battery, for the SMPS, and for the SP-AMS are from tests 1, 3 and 5 because the data is not available for the tests 2 and 4.

3. Results and discussion

3.1. Regulated emissions

European emission standards for new non-road mobile machinery include limits for gaseous emissions (CO, HC, NO_x), particulate matter, and the number of non-volatile particles with diameters over 23 nm ($PN_{>23\ nm\ non\text{-}volatile}$). These regulated emissions, (calculated according to instructions in Commission delegated regulation (EU) 2017/654 [30]), are presented in Table 3 for the prototype non-road gas engine used in this study. Averages and standard deviations were calculated from tests 1–2 with a TWC and from tests 3–5 without a TWC.

The engine produced gaseous and particulate phase pollutants, as shown in Table 3. The average engine-out emissions were on relatively similar levels for different gaseous pollutants; 10.69 g/kWh, 5.92 g/kWh and 12.6 g/kWh for CO, HC, and NO_x, respectively, but the variation (standard deviation/value) was different between these components, being 0.6%, 29.2%, and 4.0% respectively. This indicates that the CO emissions were more stable between tests, whereas larger variations existed in HC emissions.

The TWC removed the vast majority of the gaseous emissions (96% CO, 98% HC, 98% NO_x, Table 3). There were, however, some differences observed depending on the engine load point. Due to the high lambda value in mode 4 of test 1, the TWC was not working as intended, which resulted in high NO_x emissions in that mode. HC emissions were also high in this mode, possibly due to high amount of unburned lubricating oil. The engine was adjusted for test 2 when the TWC then removed pollutants more effectively in all modes of the test cycle. However, the effect of test 1 can be seen as a large standard deviation for the HC and NO_x emissions with the TWC.

The engine-out PM emissions for the prototype engine were 53 mg/kWh. The TWC removed a significant part of PM emissions (89%). Although the TWC had a major effect on the PM determined with the gravimetric method, it was observed that the non-volatile PN emissions were not significantly affected by the application of the TWC; the PN level was measured to be about 10.0×10^{12} 1/kWh both with and without the TWC. Henceforth, this, together with more detailed particle measurements discussed below, implies that the TWC efficiently reduced compounds that are in the gaseous phase at TWC temperatures. These gaseous compounds may later participate in gas-to-particle conversion when the exhaust is diluted and cooled and thus contribute to the fresh exhaust particle emissions.

3.2. Particle number emissions

Detailed particle number emission characterization was done by comparing particle number concentrations measured by parallel CPCs

Table 3
Regulated emissions and standard deviations for CO (g/kWh), HC (g/kWh), NO_x (g/kWh), PM (g/kWh), and PN (1/kWh) from the studied prototype non-road gas engine.

Compound	Without a TWC	With a TWC	TWC removal efficiency	Unit
CO	10.69 ± 0.06	0.46 ± 0.02	95.7%	g/
HC	5.92 ± 1.73	0.13 ± 0.12	97.8%	kWh
NOx	12.6 ± 0.5	0.3 ± 0.3	97.6%	
PM	0.053 ± 0.017	0.006 ± 0.002	88.7%	
$PN_{>23\ nm\ non\text{-}volatile}$	$9.42 \times 10^{12} \pm 1.54 \times 10^{12}$	$9.99 \times 10^{12} \pm 0.58 \times 10^{12}$	−6.0%	1/ kWh

with several different cut-off sizes (>1.2 nm, 2.5 nm, 5 nm, 10 nm, 23 nm), i.e., by the CPC battery. These CPCs were used to measure the exhaust sample downstream the PTD sampling system. Thus, the data measured with these instruments represents the particle number concentrations of fresh exhaust [41], meaning the situation when the initially hot exhaust has cooled and diluted and the condensable compounds of exhaust have condensed or nucleated to particle phase [42]. In addition, one CPC with a cut-off size 23 nm was used to measure the exhaust non-volatile PN downstream of the PMP sampling and exhaust treatment system. Particle number emission results are presented in Fig. 2, corrected for DR and averaged for the last 5 min of each engine load mode to avoid the effect of mode changes on the reported values. Emission factors were calculated by adapting the instructions in [30], as presented in supplementary material.

In general, the measured particle number emission factors were highly dependent on the cut-off sizes of the CPCs. Using CPCs with smaller cut-off sizes resulted in higher particle number emission factors. For instance, when the engine was operated during mode 2 with the TWC, a more than a hundredfold difference in particle number emission factors was observed between the measurements with CPCs having cut-off sizes of 1.2 nm and 23 nm, although the same exhaust sampling and dilution system was used for both of those instruments. Large differences between the results obtained with the different CPCs indicate that large fractions of the exhaust particle size distributions are found for particle sizes below 23 nm. The change of exhaust sampling and dilution system from the PTD system to PMP system (which only counts non-volatile particles) made the difference even larger, even though similar CPCs with cut-off sizes at 23 nm were used in both systems. The results show that the PMP system measures only a very minor part of the particle emissions. Furthermore, it seems that even the proposed 10 nm size limit leaves large fractions of the particles undetected, especially downstream the TWC. In addition to the cut-off size of the CPC and the exhaust sampling and dilution system, the engine load also significantly affected the particle number emissions of the test engine. This can be seen in Fig. 2 as a decrease in particle number emissions as a function of decreasing torque in modes 1–3 and in modes 5–7, both with and without the TWC, and with all instruments. The effect was large especially when the engine was running at an intermediate speed, i.e., during modes 5–7. The highest particle number emissions were observed during the idling modes 4 and 8. However, this was partly due to the small work during these modes and not observed in time-based emissions (Figure S3).

There was a large difference in particle number emissions after the TWC (Fig. 2, right vs. left panel). The use of the TWC led to a greater portion of small particles, because the number emissions of larger particles were reduced. This is seen especially in the (>10 nm) and (>23 nm) results. Since the total particle number concentration (>1.2 nm) was relatively independent of the use of the TWC, it can be estimated that this size reduction over the TWC is caused by semi-volatile components whose concentrations are reduced in the exhaust downstream the TWC, which reduces the amount of material that can absorb onto particles to produce larger particles.

During the tests, the engine operation modes lasted 10 min according to the regulated minimum mode length [30]. Fig. 3 shows that in mode 1 of NRSC the $PN_{>23\ nm\ non\text{-}volatile}$ exhibits wavelike behavior throughout the 10-minute mode. There is no great difference in $PN_{>23\ nm\ non\text{-}volatile}$ between tests with (1–2) or without (3–5) a TWC. This wavelike behavior correlates well with BC emissions, as is discussed later in

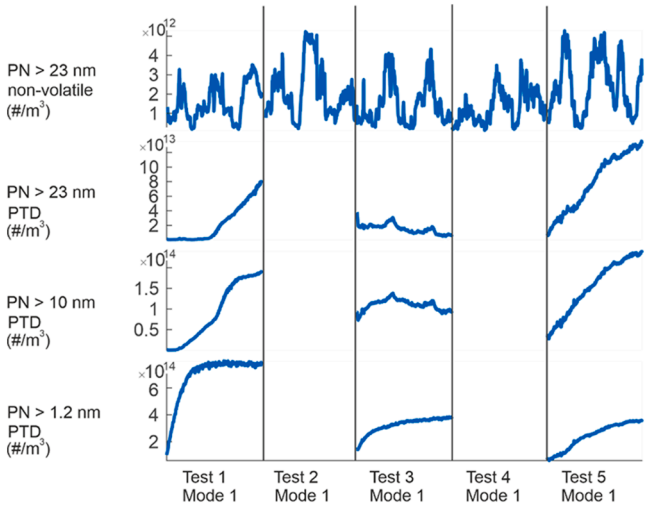

Fig. 3. Comparison of particle number concentrations as a function of time either applying the PMP method or downstream the PTD sampling system that allows gas-to-particle conversion processes. Complete 10-minute segments for mode 1 from tests 1–5 are presented side by side.

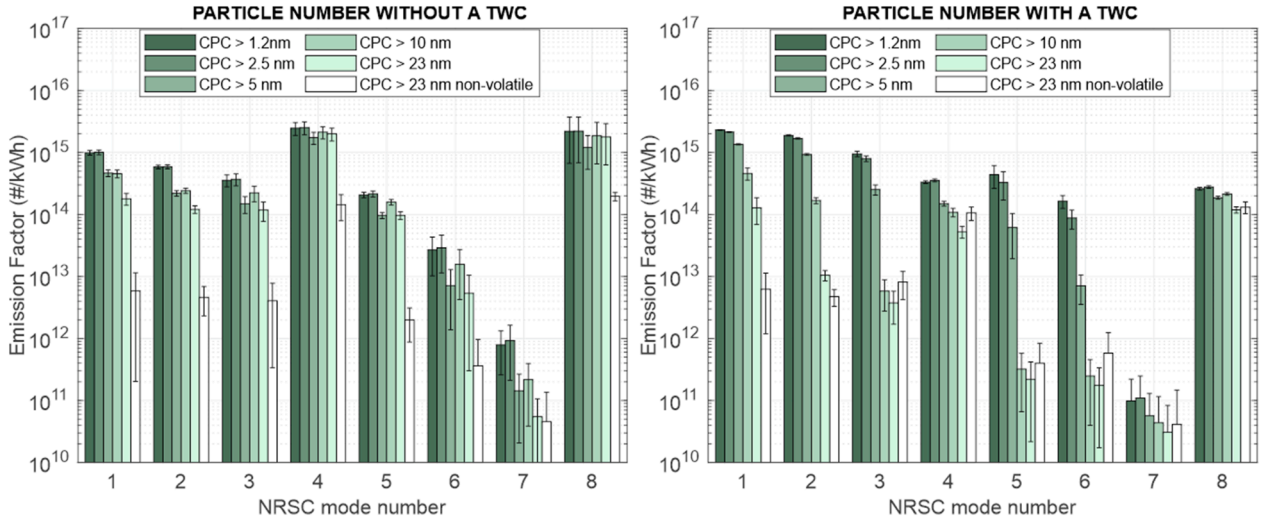

Fig. 2. Particle number emission factors (#/kWh) without (left) and with (right) a three-way catalyst for 8 modes of the NRSC cycle with 6 different particle number instruments. CPC > 23 nm non-volatile particles were measured applying the PMP protocol downstream of CVS dilution (rightmost, white bars), while the 5 other number concentrations were measured downstream of the PTD system (colored bars). Concentrations were corrected for the DR and averaged for the last 5 min of the 10-minute mode. Note the logarithmic scale.

section 3.4. However, it could be observed that the 10-minute mode was not always sufficiently long to allow the concentrations to stabilize downstream the PTD sampling system that enables gas-to-particle conversion processes (example shown in Fig. 3). For this reason, only the last 5 min of the modes were averaged to produce the emission results (Fig. 2).

In test 1, it could be seen that the rapid increase and stabilization in $PN_{>1.2\ nm}$ was followed by corresponding increases first in $PN_{>10\ nm}$ and then $PN_{>23\ nm}$. The observed behavior may be linked to changes in the TWC temperature (Figure S1), resulting in formation of new particles through sulfuric acid nucleation (see e.g. [43,44]). The behavior of $PN_{>10\ nm}$ and $PN_{>23\ nm}$ differed greatly in the tests without TWC (tests 3 and 5), while $PN_{>\ 1.2\ nm}$ behaved quite similarly. This corresponds to greater average particle sizes in test 5, as is discussed below. Overall, Fig. 3 gives an indication that the particle levels produced by the engine are not always stable as a function of time. Changes in solid particles could be caused by changes in air-to-fuel ratio, lubricating oil infusion, and temperatures. Fig. 3 also indicates that especially the stabilization and growth of nucleation mode particles, which include semi-volatile material, may require longer sampling times.

3.3. Particle number size distributions

Particle number size distributions are presented in Fig. 4 with and without the TWC installed downstream the engine. The results are corrected for the DR and averaged for the last 4 complete Nano-SMPS scans for each mode, which represents approximately the last 5 min of each mode. For results without TWC, distributions from test 3 and 5 are presented independently because they cannot be averaged without giving the impression that several particle modes are forming simultaneously. Particle size distribution data with other data presented in this article suggest that the nucleation mode particles grew to larger sizes during test 5 compared to test 3.

Overall, the results from tests without the TWC showed that the concentration and size of nucleation mode particles varied strongly depending on the engine operation mode. This observable nucleation mode was constantly present, except in mode 7, which corresponds to medium load with intermediate engine speed. In modes 4 and 8, the mean particle size was especially large at around 50 nm, and at first glance they would appear as typical soot particles seen in the accumulation mode. However, chemical composition of the particles, discussed later, indicates that they originate from organic compounds. Overall, it can be said that without a TWC, there seems to be a shift to smaller particle sizes as the engine torque goes down, (comparing between modes 5–7 or between modes 1–3).

The particle number size distributions for the test with the TWC show a greater share of small particles. Especially for the intermediate speed (modes 5–7), the peaks of the distributions are already below 4 nm, which was the cut-off size of the Nano-SMPS. It seems that the formation of particles larger than 50 nm, observed in other engine modes, is not observed in modes 5–7. Our interpretation is that the soot particles are shown in the particle size distribution modes with the largest particle sizes, and during most of the engine operation modes, there is enough available material for nucleation mode particles to grow to larger sizes,

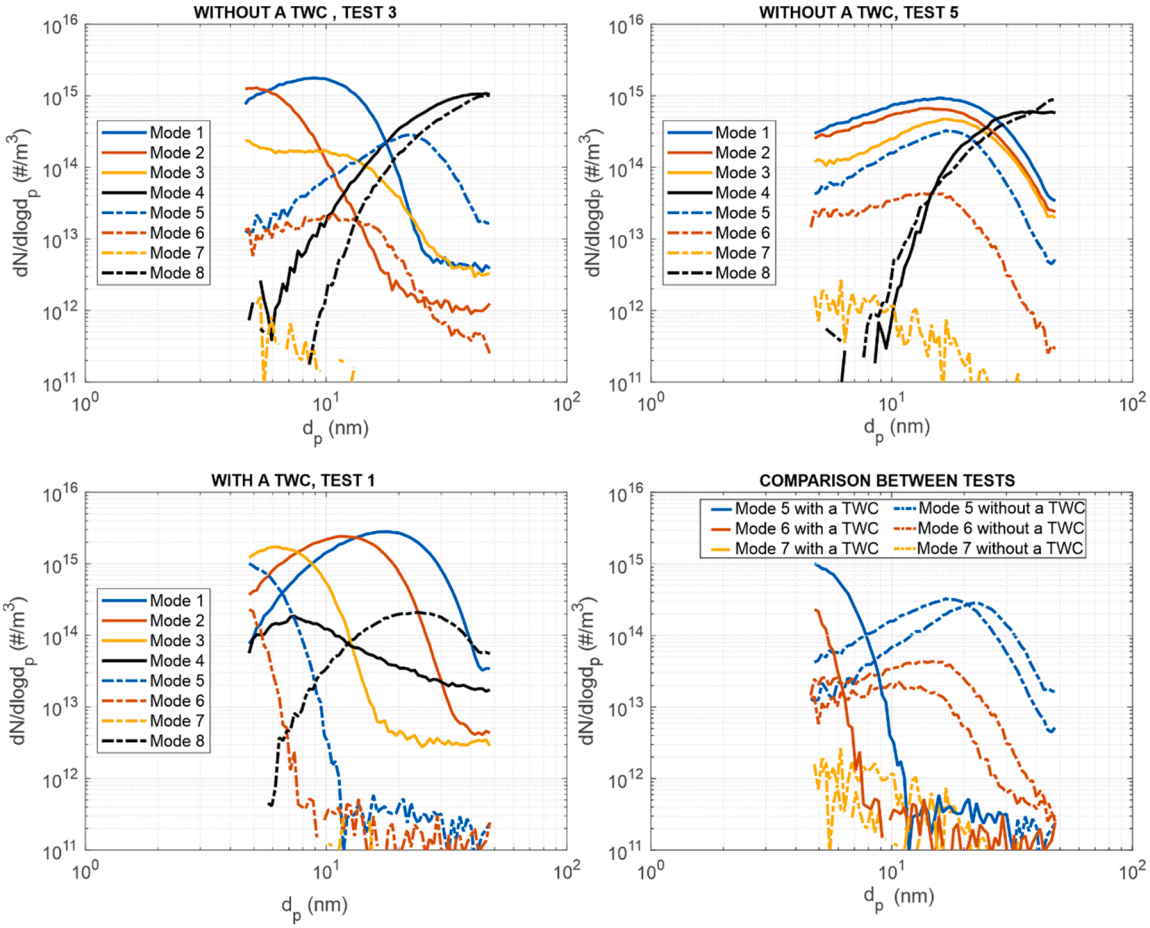

Fig. 4. Mean exhaust particle number size distributions for 8 modes of NRSC from tests 3 and 5 without a three-way catalyst (top) and from test 1 with a TWC (bottom left) calculated from Nano-SMPS data. Tests 3 and 5 are presented independently as they show the nucleation mode at different particle sizes. Results were corrected for the DR and averaged over the last 4 complete scans, approximately last 5 min, of each mode. The bottom right figure, where results for Modes 5–7 are shown with and without TWC, illustrates an example of the effect of TWC on particle number size distribution.

as shown in Fig. 4 for the without TWC tests. For the test with the TWC, the precursor gases were significantly reduced due to oxidation in the TWC, which significantly reduced particles above 50–60 nm size, as can be observed from the particle number size distributions, especially in modes 5–7 (example in Fig. 4).

3.4. Black carbon emissions

BC emissions were measured with five different instruments over the eight steady operating modes with and without a TWC. BC emission factors for each mode were calculated in the same way as presented in section 3.2 for particle number. BC emission factors are presented in Fig. 5. The results were corrected for the DR and averaged for the last five minutes of the 10-minute mode.

Fig. 5 shows that modes 5–7 with the intermediate engine speed led to lower BC emissions than modes 1–3. This result is intuitive since with lower speeds there should be more time for soot oxidation during the combustion cycle. Mode 4 and mode 8, which represent idle conditions with very low torque, lead to a great increase in BC emissions by over one order of magnitude. BC emissions were highest in these modes also when considering time-based emissions (Figure S3), although the increase was not as significant. In previous studies, CNG engines have been observed to exhibit increased particle emissions especially during accelerations following a long period of idling, which has been suggested to result from lubricating oil infusion. Lubricating oil can enhance soot precursor formation inside the cylinder and undergo pyrolysis or partial oxidation in the exhaust gases [45]. The TWC didn't significantly affect the BC emission factors.

The BC emission factors measured by several different methods were in most cases within one standard deviation. This was especially true for the instruments based on optical measurement methods (AE33, MA200, and MAAP). The results given by the optical instruments were slightly higher than results given by the photoacoustic method (MSS), which can result from the different measurement principles or possibly interference of semi-volatile species, which can be present on the surface of BC particles after PTD dilution. The largest difference was seen in the emission factors measured by the SP-AMS, which measures the mass of refractory carbon in the particles. Additionally, the size range of the SP-AMS is limited to approximately 50 nm − 1 μm particles.

The wavelike behavior of $PN_{>23\ nm\ non\text{-}volatile}$ particles in mode 1 (see Fig. 6) was also observed for BC emissions. Despite the different dilution methods between the instruments, correlation between BC and $PN_{>23\ nm\ non\text{-}volatile}$ is good overall (Fig. 6 and Figure S2). This may indicate that reductions targeted to $PN_{>23\ nm\ non\text{-}volatile}$ could also help combat BC emissions from gas engines.

3.5. Chemical composition

The chemical composition of submicron particle emissions with and without a TWC was studied with a SP-AMS. Results are presented in Fig. 7, corrected for the DR and averaged for the last 5 min of each 10-minute mode.

Without a TWC, the chemical composition of the exhaust particles was dominated by organics, with a contribution from 71 to up to 100%. The lowest organic contributions (71–74%) were found for modes 6 and 7. For modes 3 and 5, the contribution of organics was larger (~95%), and for modes 4 and 8 only organic compounds were detected by the aerosol mass spectrometer. A composition that is dominated by organic compounds in modes 4 and 8 indicates that the particles observed in Fig. 4 around 50–60 nm mainly include large nucleation mode particles in addition to BC.

With a TWC the composition of exhaust PM was very different. The contribution of organics remained high for mode 8, with a contribution over 90%, and for modes 3, 4, and 6 the contribution was >50%. The largest reductions for organics were observed for modes 4 and 8. For modes 1 and 2, the submicron PM mass was dominated by sulfate, likely originating from the lubricating oil. For modes 5 and 7, the submicron PM was dominated by BC (contribution ~50–70%). The BC forms in incomplete combustion and may suggest unoptimal burning conditions.

The origin and characteristics of PM with and without the TWC were investigated by applying the PMF method to the mass spectra measured by the SP-AMS. The results from the PMF analysis are shown in Fig. 8. Two different types of organics were found both without and with the TWC, suggesting that PM_1 emitted by the gas engine had two major origins. All factors were dominated by hydrocarbon fragments and are therefore called generically hydrocarbon-like organic aerosols. HOA-1a and HOA-2a mark the factors obtained without the TWC and HOA-1b and HOA-2b the factors obtained with the TWC. Without the TWC, organics were dominated by HOA-1a, but in modes 4 and 8 the majority of organics were composed of HOA-2a. HOA-1a and HOA-2a had very similar mass spectra, with the largest signal for $C_4H_9^+$ (m/z 57) followed by $C_3H_5^+$ (m/z 41), $C_3H_7^+$ (m/z 43) and $C_4H_7^+$ (m/z 55) and $C_5H_{11}^+$ (m/z 71). However, HOA-2a had slightly larger contribution of saturated hydrocarbons i.e., the ratio of $C_3H_7^+$ to $C_3H_5^+$ and $C_4H_9^+$ to $C_4H_7^+$ was larger than for HOA-1a. Both HOA-1a and HOA-2a had only a minor fraction of organic fragments with oxygen. In terms of inorganics, BC, sulfate, and zinc were associated with both HOA-1a and HOA-2a, but their contribution was much larger in HOA-1a. Based on the chemical

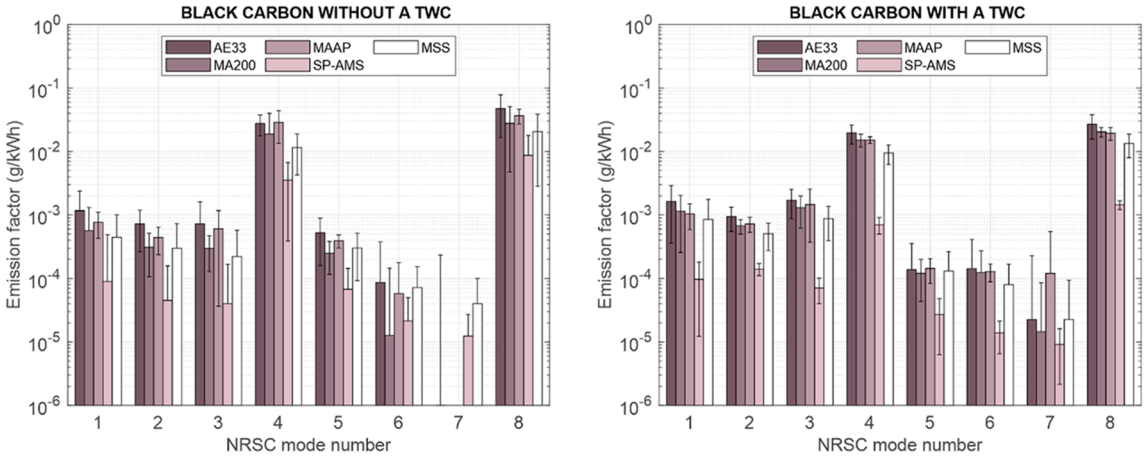

Fig. 5. BC emission factors without (left) and with (right) a three-way catalyst for 8 modes of the NRSC cycle with 5 different BC measuring instruments. The MSS (rightmost, white bars) measured from the undiluted exhaust after heated sampling lines using photoacoustic principles, while the 4 other instruments (colored bars) measured downstream of the PTD sampling system. AE33, MA200, and MAAP measure optically. SP-AMS measures the refractory black carbon. Results were corrected for the DR and averaged for the last 5 min of the 10-minute mode. Note the logarithmic scale.

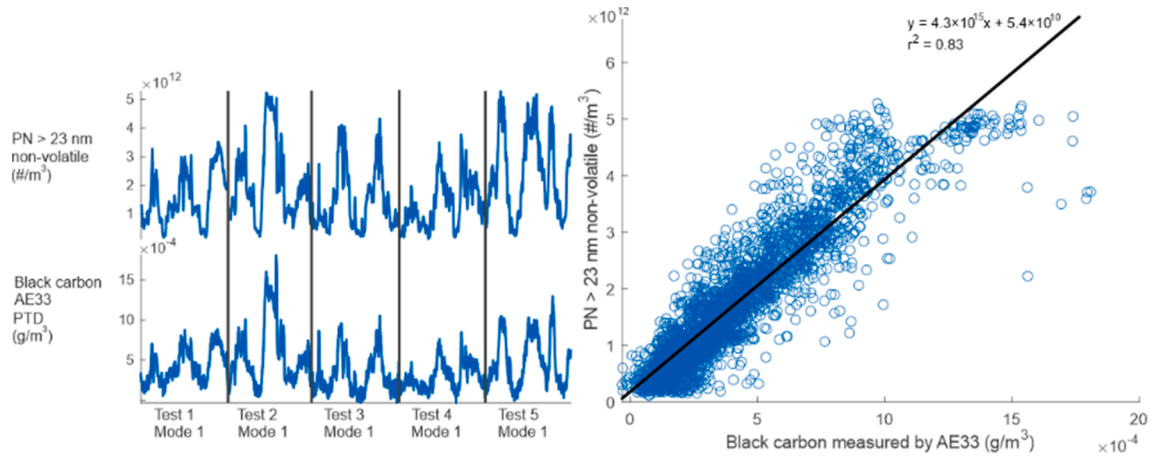

Fig. 6. Wavelike behavior of particle number $PN_{>23\ nm\ non\text{-}volatile}$ and BC as a function of time for mode 1 of tests 1–5 (left). Scatterplot with a fitted polynomial of particle number and BC data from mode 1 of tests 1–5 (right).

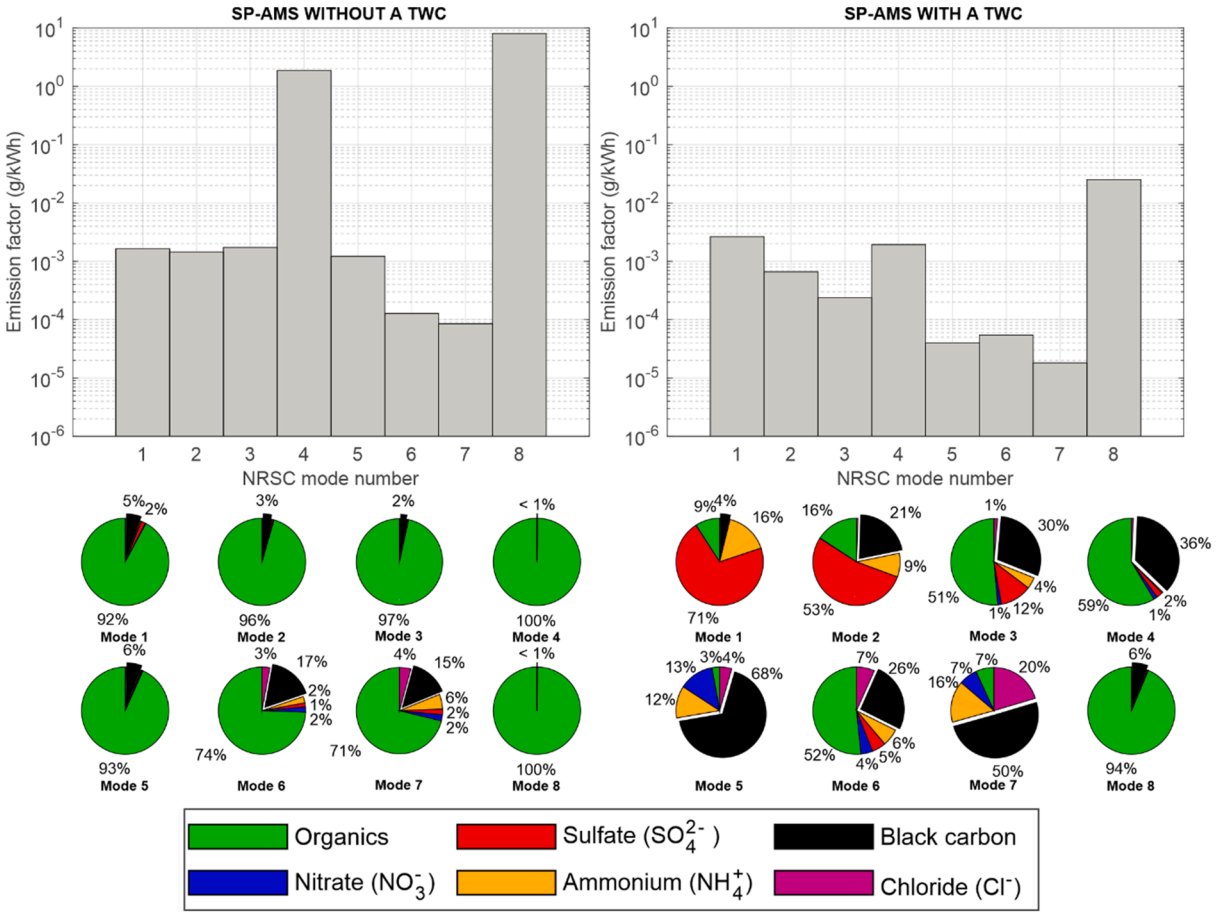

Fig. 7. Average PM_1 emission factors (top panels) and concentration based chemical composition (bottom panels) of submicron particles without (left) and with (right) a TWC for different modes (1–8) measured with a SP-AMS.

composition, both HOAs were likely related to lubricating oil, but because of the much larger contribution of BC in HOA-1a, HOA-1a was likely to be related to combusted lubricating oil, whereas HOA-2a consisted of unburnt lubricating oil.

Similar to the measurements without the TWC, for the TWC measurements, both types of organics (HOA-1b and HOA-2b) consisted mostly of hydrocarbon fragments. Organics in modes 1–7 were dominated by HOA-1b that had some similarities in the mass spectra to HOA-1a and HOA-2a measured without the TWC. Since BC was mostly attributed to HOA-1b, HOA-1b was assumed to be related to combusted lubricating oil. However, with the TWC, combusted lubricating oil particles were more oxygenated than without the TWC, as the oxygen-to-carbon ratio (O:C) for organics increased from 0.002 without the TWC to 0.1 with the TWC. In mode 8, 99% of organics were associated with HOA-2b that was assumed to be related to unburnt lubricating oil. Compared to the mass spectra of unburnt lubricating oil without the TWC (HOA-2a), HOA-2b had more signal at smaller *m/z*s, with $C_3H_5^+$ (*m/z* 41) being the dominant hydrocarbon fragment followed by $C_3H_3^+$

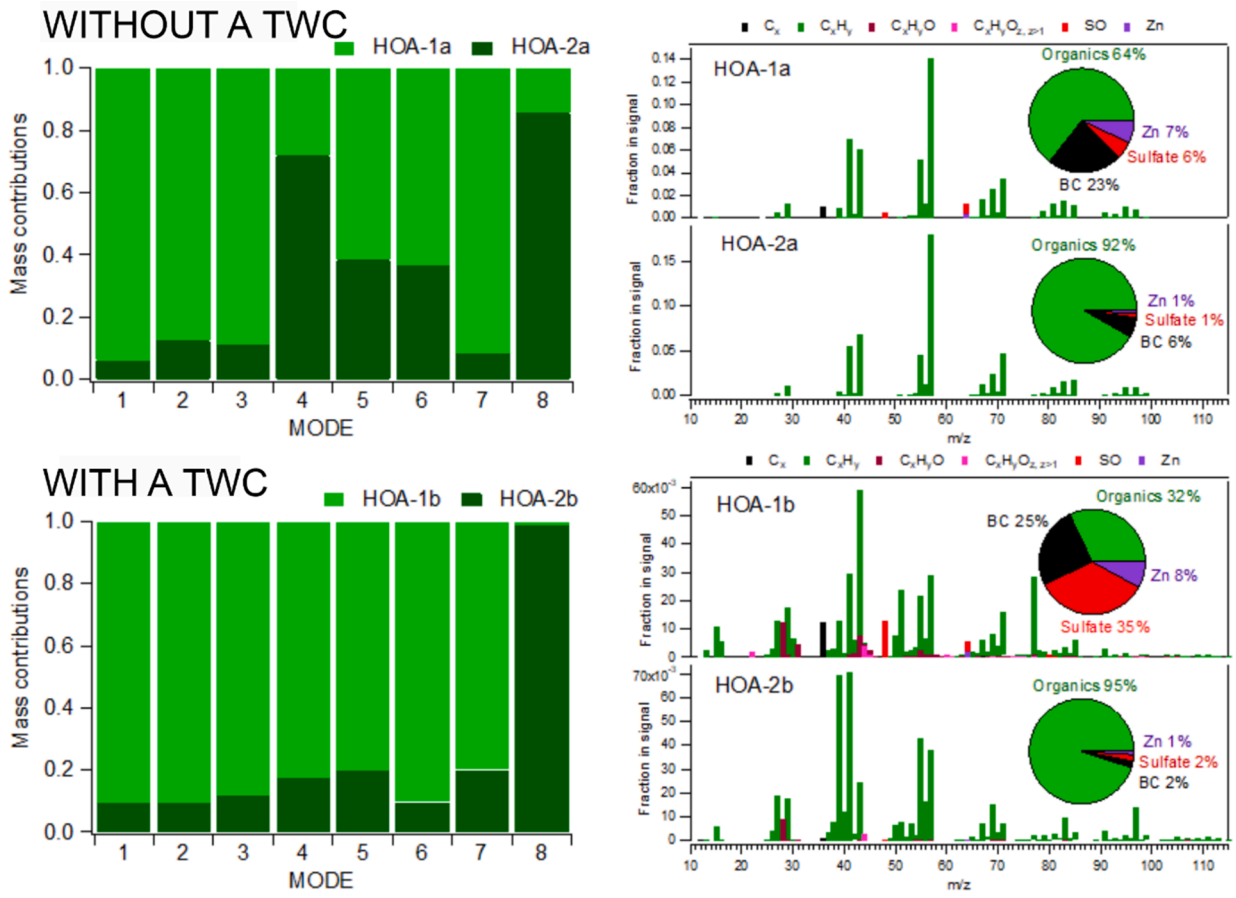

Fig. 8. Source apportionment (PMF) results for submicron particles without (top) and with (bottom) a TWC measured with SP-AMS. PMF analysis was performed separately for the data measured without the TWC (factors HOA-1a and HOA-2a) and with the TWC (factors HOA-1b and HOA-2b). Pie plots show only the chemical species used in the PMF analysis. Relative ionization efficiencies of 0.1, 1.2 and 1 were utilized for BC, sulfate, and zinc, respectively.

(*m/z* 39). Additionally, unburnt lubricating oil particles were much more oxygenated after the TWC since O:C increased from 0.0005 (without the TWC) to 0.025 (with the TWC).

4. Conclusions

Particle and gaseous emissions were investigated from a non-road natural gas engine. The engine applied spark plugs to ignite premixed natural gas and was equipped with a TWC. Tests with and without the TWC installed demonstrated that the TWC efficiently reduced the regulated gaseous and particulate mass emissions (96% CO, 98% HC, 98% NO_x, 98% PM) from this natural gas engine, but $PN_{>23\ nm\ non\text{-}volatile}$ emissions were not significantly reduced. In general, the measured particle number emission factors for all particles, including volatile species, were highly dependent on the cut-off sizes of the CPCs, and the results show that a significant fraction of these particles may remain undetected when cut-points above 23 nm, or even above 10 nm cut-point are applied.

The BC emission factors were not influenced by the TWC but were generally low compared to other combustion emission sources without filtration. BC emissions were lowest during modes with the intermediate engine speed. In contrast, idling produced the highest BC emissions.

The chemical composition of the particles measured by aerosol mass spectrometry showed that the particle composition depended on the engine operation condition, and the majority of particles were comprised of either sulfate, BC, or organic compounds. Without the TWC, organic compounds dominated the particle composition. The positive matrix factorization of the aerosol mass spectra suggested two sources for the particle mass, unburned and combusted lubricating oil. Particles originated directly from natural gas combustion are likely very small in diameter and have a minor contribution to the particle mass measured by the SP-AMS because of losses in the instrument for particles with diameter <50 nm. Similar characterization and tracing the sources of gaseous HC emissions, for example with chemical ionization mass spectrometry, should be a topic for future studies of gas-fueled engines.

CRediT authorship contribution statement

Petteri Marjanen: Conceptualization, Methodology, Validation, Formal analysis, Investigation, Writing – original draft, Visualization. **Niina Kuittinen:** Conceptualization, Methodology, Investigation, Writing – original draft, Project administration. **Panu Karjalainen:** Conceptualization, Writing – original draft, Visualization, Supervision, Project administration, Funding acquisition. **Sanna Saarikoski:** Conceptualization, Formal analysis, Investigation, Writing – original draft, Visualization. **Mårten Westerholm:** Methodology, Validation, Formal analysis, Investigation, Writing – review & editing. **Rasmus Pettinen:** Conceptualization, Methodology, Investigation, Writing – review & editing. **Minna Aurela:** Investigation, Writing – review & editing. **Henna Lintusaari:** Investigation, Writing – review & editing. **Pauli Simonen:** Investigation, Writing – review & editing. **Lassi Markkula:** Investigation, Writing – review & editing. **Joni Kalliokoski:** Conceptualization, Methodology. **Hugo Wihersaari:** Conceptualization, Writing – original draft, Writing – review & editing. **Hilkka Timonen:** Conceptualization, Resources, Writing – original draft, Supervision, Project administration, Funding acquisition. **Topi Rönkkö:** Conceptualization, Resources, Writing – original draft, Supervision, Project administration, Funding acquisition.

Declaration of Competing Interest

The authors declare that they have no known competing financial interests or personal relationships that could have appeared to influence the work reported in this paper.

Acknowledgements

This work was supported by the BC Footprint project funded by Business Finland, participating companies and municipalities (Grant number: 530/31/2019 and 528/31/2019), and Academy of Finland Flagship funding (grant no's. 337551 and 337552). P.K. acknowledges Academy of Finland project "EFFi" grant Nr. 322120. We thank Leonardo Oliveira de Negri for his help with the aerosol measurements.

Appendix A. Supplementary data

Supplementary data to this article can be found online at https://doi.org/10.1016/j.fuel.2022.123387.

References

[1] IPCC. Climate Change 2014: Synthesis Report. Contribution of Working Groups I, II and III to the Fifth Assessment Report of the Intergovernmental Panel on Climate Change [Core Writing Team, R.K. Pachauri and L.A. Meyer (eds.)]. 2014. https://doi.org/10.1017/CBO9781139177245.003.
[2] Backman J, Schmeisser L, Asmi E. Asian emissions explain much of the arctic black carbon events. Geophys Res Lett 2021;48(5). https://doi.org/10.1029/2020GL091913.
[3] Bond TC, Doherty SJ, Fahey DW, Forster PM, Berntsen T, DeAngelo BJ, et al. Bounding the role of black carbon in the climate system: a scientific assessment. J Geophys Res Atmos 2013;118(11):5380–552. https://doi.org/10.1002/jgrd.50171.
[4] Cape JN, Coyle M, Dumitrean P. The atmospheric lifetime of black carbon. Atmos Environ 2012;59:256–63. https://doi.org/10.1016/j.atmosenv.2012.05.030.
[5] Kühn T, Kupiainen K, Miinalainen T, Kokkola H, Paunu V-V, Laakso A, et al. Effects of black carbon mitigation on Arctic climate. Atmos Chem Phys 2020;20(9):5527–46. https://doi.org/10.5194/acp-20-5527-2020.
[6] Sand M, Berntsen TK, Ekman AML, Hansson H-C, Lewinschal A. Surface temperature response to regional black carbon emissions: Do location and magnitude matter-. Atmos Chem Phys 2020;20(5):3079–89. https://doi.org/10.5194/acp-20-3079-2020.
[7] Lähde T, Rönkkö T, Virtanen A, Solla A, Kytö M, Söderström C, et al. Dependence between nonvolatile nucleation mode particle and soot number concentrations in an EGR equipped heavy-duty diesel engine exhaust. Environ Sci Technol 2010;44(8):3175–80. https://doi.org/10.1021/es903428y.
[8] Wihersaari H, Pirjola L, Karjalainen P, Saukko E, Kuuluvainen H, Kulmala K, et al. Particulate emissions of a modern diesel passenger car under laboratory and real-world transient driving conditions. Environ Pollut 2020;265:114948. https://doi.org/10.1016/j.envpol.2020.114948.
[9] Jang, J. Lee, Y., Kwon O. Comparison of fuel efficiency and exhaust emissions between the aged and new DPF systems of EURO 5 diesel passenger car. Int J Automot Technol 2017;18:751–8. 10.1007/s12239−017−0074−9.
[10] Timonen H, Karjalainen P, Aalto P, Saarikoski S, Mylläri F, Karvosenoja N, et al. Adaptation of black carbon footprint concept would accelerate mitigation of global warming. Environ Sci Technol 2019;53(21):12153–5. https://doi.org/10.1021/acs.est.9b05586.
[11] Grahame TJ, Klemm R, Schlesinger RB. Public health and components of particulate matter: the changing assessment of black carbon. J Air Waste Manag Assoc 2014;64(6):620–60. https://doi.org/10.1080/10962247.2014.912692.
[12] Janssen NAH, Hoek G, Simic-Lawson M, Fischer P, van Bree L, ten Brink H, et al. Black carbon as an additional indicator of the adverse health effects of airborne particles compared with pm10 and pm2.5. Environ Health Perspect 2011;119(12):1691–9. https://doi.org/10.1289/ehp.1003369.
[13] Luben TJ, Nichols JL, Dutton SJ, Kirrane E, Owens EO, Datko-Williams L, et al. A systematic review of cardiovascular emergency department visits, hospital admissions and mortality associated with ambient black carbon. Environ Int 2017;107:154–62. https://doi.org/10.1016/j.envint.2017.07.005.
[14] Cho HM, He B-Q. Spark ignition natural gas engines-a review. Energy Convers Manag 2007;48(2):608–18. https://doi.org/10.1016/j.enconman.2006.05.023.
[15] Knudsen MT, Meyer-Aurich A, Olesen JE, Chirinda N, Hermansen JE. Carbon footprints of crops from organic and conventional arable crop rotations – using a life cycle assessment approach. J Clean Prod 2014;64:609–18. https://doi.org/10.1016/j.jclepro.2013.07.009.
[16] Watne ÅK, Psichoudaki M, Ljungström E, Le Breton M, Hallquist M, Jerksjö M, et al. Fresh and oxidized emissions from in-use transit buses running on diesel, biodiesel, and CNG. Environ Sci Technol 2018;52(14):7720–8. https://doi.org/10.1021/acs.est.8b01394.
[17] Jayaratne ER, Ristovski ZD, Meyer N, Morawska L. Particle and gaseous emissions from compressed natural gas and ultralow sulphur diesel-fuelled buses at four steady engine loads. Sci Total Environ 2009;407(8):2845–52. https://doi.org/10.1016/j.scitotenv.2009.01.001.
[18] Aakko-Saksa P, Koponen P, Roslund P, Laurikko J, Nylund N-O, Karjalainen P, et al. Comprehensive emission characterisation of exhaust from alternative fuelled cars. Atmos Environ 2020;236:117643. https://doi.org/10.1016/j.atmosenv.2020.117643.
[19] Saarikoski S, Timonen H, Carbone S, Kuuluvainen H, Niemi JV, Kousa A, et al. Investigating the chemical species in submicron particles emitted by city buses. Aerosol Sci Technol 2017;51(3):317–29. https://doi.org/10.1080/02786826.2016.1261992.
[20] Pope CA, Dockery DW. Health effects of fine particulate air pollution: Lines that connect. J Air Waste Manag Assoc 2006;56(6):709–42. https://doi.org/10.1080/10473289.2006.10464485.
[21] Lelieveld J, Evans JS, Fnais M, Giannadaki D, Pozzer A. The contribution of outdoor air pollution sources to premature mortality on a global scale. Nature 2015;525(7569):367–71. https://doi.org/10.1038/nature15371.
[22] Sofiev M, Winebrake JJ, Johansson L, Carr EW, Prank M, Soares J, et al. Cleaner fuels for ships provide public health benefits with climate tradeoffs. Nat Commun 2018;9(1). https://doi.org/10.1038/s41467-017-02774-9.
[23] Pirjola L, Dittrich A, Niemi JV, Saarikoski S, Timonen H, Kuuluvainen H, et al. Physical and chemical characterization of real-world particle number and mass emissions from city buses in Finland. Environ Sci Technol 2016;50(1):294–304. https://doi.org/10.1021/acs.est.5b04105.
[24] Alanen J, Isotalo M, Kuittinen N, Simonen P, Martikainen S, Kuuluvainen H, et al. Physical characteristics of particle emissions from a medium speed ship engine fueled with natural gas and low-sulfur liquid fuels. Environ Sci Technol 2020;54(9):5376–84. https://doi.org/10.1021/acs.est.9b06460.
[25] Alanen J, Saukko E, Lehtoranta K, Murtonen T, Timonen H, Hillamo R, et al. The formation and physical properties of the particle emissions from a natural gas engine. Fuel 2015;162:155–61. https://doi.org/10.1016/j.fuel.2015.09.003.
[26] Alanen J, Simonen P, Saarikoski S, Timonen H, Kangasniemi O, Saukko E, et al. Comparison of primary and secondary particle formation from natural gas engine exhaust and of their volatility characteristics. Atmos Chem Phys Discuss 2017:1–27. https://doi.org/10.5194/acp-2017-44.
[27] Lehtoranta K, Aakko-Saksa P, Murtonen T, Vesala H, Ntziachristos L, Rönkkö T, et al. Particulate mass and non-volatile particle number emissions from marine engines using low-sulfur fuels, natural gas or scrubbers. Submitt to Environ Sci Technol 2019;53(6):3315–22. https://doi.org/10.1021/acs.est.8b05555.
[28] McCaffery C, Zhu H, Tang T, Li C, Karavalakis G, Cao S, et al. Real-world NOx emissions from heavy-duty diesel, natural gas, and diesel hybrid electric vehicles of different vocations on California roadways. Sci Total Environ 2021;784:147224. https://doi.org/10.1016/j.scitotenv.2021.147224.
[29] Kuittinen N, Jalkanen J-P, Alanen J, Ntziachristos L, Hannuniemi H, Johansson L, et al. Shipping Remains a Globally Significant Source of Anthropogenic PN Emissions even after 2020 Sulfur Regulation. Environ Sci Technol 2021;55(1):129–38. https://doi.org/10.1021/acs.est.0c0362710.1021/acs.est.0c03627.s001.
[30] Commission delegated regulation (EU) 2017/654 2017.
[31] Ntziachristos L, Giechaskiel B, Pistikopoulos P, Samaras Z, Mathis U, Mohr M, et al. Performance evaluation of a novel sampling particle characterization. Engineering 2004;2004.
[32] Mikkanen P, Moisio M. Sampling Method for Particle Measurements of Vehicle Exhaust 2001:1–6.
[33] Bergmann M, Vogt R, Szente J, Maricq M, Benter T. Using ejector diluters to sample vehicle exhaust at elevated pressures and temperatures. SAE Int J Engines 2009;1(1):1167–78. https://doi.org/10.4271/2008-01-2434.
[34] Rönkkö T, Virtanen A, Vaaraslahti K, Keskinen J, Pirjola L, Lappi M. Effect of dilution conditions and driving parameters on nucleation mode particles in diesel exhaust: laboratory and on-road study. Atmos Environ 2006;40(16):2893–901. https://doi.org/10.1016/j.atmosenv.2006.01.002.
[35] Hering SV, Spielman SR, Lewis GS. Moderated, water-based, condensational particle growth in a laminar flow. Aerosol Sci Technol 2014;48(4):401–8. https://doi.org/10.1080/02786826.2014.881460.
[36] Onasch TB, Trimborn A, Fortner EC, Jayne JT, Kok GL, Williams LR, et al. Soot particle aerosol mass spectrometer: development, validation, and initial application. Aerosol Sci Technol 2012;46(7):804–17. https://doi.org/10.1080/02786826.2012.663948.
[37] Paatero P, Tapper U. Positive matrix factorization: a non-negative factor model with optimal utilization of error estimates of data values. Environmetrics 1994;5(2):111–26. https://doi.org/10.1002/env.3170050203.
[38] Ulbrich IM, Canagaratna MR, Zhang Q, Worsnop DR, Jimenez JL. Interpretation of organic components from Positive Matrix Factorization of aerosol mass spectrometric data. Atmos Chem Phys 2009;9(9):2891–918. https://doi.org/10.5194/acp-9-2891-200910.5194/acp-9-2891-2009-supplement.
[39] Carbone S, Timonen HJ, Rostedt A, Happonen M, Rönkkö T, Keskinen J, et al. Distinguishing fuel and lubricating oil combustion products in diesel engine exhaust particles. Aerosol Sci Technol 2019;53(5):594–607. https://doi.org/10.1080/02786826.2019.1584389.
[40] Rivellini L-H, Adam M, Kasthuriarachchi N, Lee A. Characterization of carbonaceous aerosols in Singapore: insight from black carbon fragments and trace metal ions detected by a soot-particle aerosol mass spectrometer. Atmos Chem Phys Discuss 2019:1–28. https://doi.org/10.5194/acp-2019-857.
[41] Rönkkö T, Timonen H. Overview of sources and characteristics of nanoparticles in urban traffic-influenced areas. J Alzheimer's Dis 2019;72(1):15–28. https://doi.org/10.3233/JAD-190170.

[42] Keskinen J, Rönkkö T. Can real-world diesel exhaust particle size distribution be reproduced in the laboratory? a critical review. J Air Waste Manag Assoc 2010;60:1245–55. https://doi.org/10.3155/1047-3289.60.10.1245.
[43] Rönkkö T, Lähde T, Heikkilä J, Pirjola L, Bauschke U, Arnold F, et al. Effects of gaseous sulphuric acid on diesel exhaust nanoparticle formation and characteristics. Environ Sci Technol 2013;47(20):11882–9. https://doi.org/10.1021/es402354y.
[44] Karjalainen P, Rönkkö T, Pirjola L, Heikkilä J, Happonen M, Arnold F, et al. Sulfur driven nucleation mode formation in diesel exhaust under transient driving conditions. Environ Sci Technol 2014;48:2336–43. https://doi.org/10.1021/es405009g.
[45] Distaso E, Amirante R, Calò G, De Palma P, Tamburrano P. Evolution of soot particle number, mass and size distribution along the exhaust line of a heavy-duty engine fueled with compressed natural gas. Energies 2020;13. https://doi.org/10.3390/en13153993.